Environmental Science and Pollution Research (2021) 28:62474–62486
https://doi.org/10.1007/s11356-021-15144-2

RESEARCH ARTICLE

Fast and efficient adsorption of palladium from aqueous solution by magnetic metal–organic framework nanocomposite modified with poly(propylene imine) dendrimer

Hossein Shahriyari Far[1] · Mahdi Hasanzadeh[2] · Mohammad Shabani Nashtaei[1] · Mahboubeh Rabbani[1]

Received: 30 March 2021 / Accepted: 22 June 2021 / Published online: 1 July 2021

Abstract

In this study, a magnetic metal–organic framework (MMOF) was synthesized and post-modified with poly(propyleneimine) dendrimer to fabricate a novel functional porous nanocomposite for adsorption and recovery of palladium (Pd(II)) from aqueous solution. The morphological and structural characteristics of the prepared material were identified by field emission scanning electron microscopy (FESEM), X-ray diffraction (XRD), Fourier transform infrared spectroscopy (FTIR), Brunauer–Emmet–Teller (BET) isotherm, and vibrating sample magnetometer (VSM). The results confirmed the successful synthesis and post-modification of MMOF. Semispherical shape particles (20–50 nm) with appropriate magnetic properties and a high specific surface area of 120 m^2/g were obtained. An experimental design approach was performed to show the effect of adsorption conditions on Pd(II) uptake efficiency of the dendrimer-modified magnetic adsorbent. The study showed that the Pd(II) uptake on dendrimer-modified MMOF was well described by the Langmuir isotherm model with the highest uptake capacity of 291 mg/g under optimal condition (adsorbent content of 12.5 mg, Pd ion concentration of 80 ppm, pH = 4, and contact time of 40 min). The adsorption kinetics of Pd(II) ions was suggested to be a pseudo-first-order model. The results revealed a faster adsorption rate and higher adsorption capacity (about 43%) for dendrimer-modified MMOF. Finally, the reusability of the provided adsorbent was evaluated. This work provides a valuable strategy for designing and developing efficient magnetic adsorbents based on MOFs for the adsorption and recovery of precious metals.

Keywords Magnetic metal–organic framework · Adsorption · Palladium · Dendrimer

Introduction

In recent years, palladium (Pd) as a precious metal has received increasing attention due to high industrial demands for jewelry, medicine, electronics, fuel cell technology, and catalysts (Mergola et al. 2020). However, the high value of Pd and its low natural abundance make its recovery and reusability economically feasible. Hence, the development of cost-effective and efficient methods for the separation and extraction of Pd from industrial wastewater has become a big concern. So far, conventional methods such as membrane separation, ion exchange, solvent extraction, adsorption, and microbiological approaches have been widely used to recover or separate Pd ion (B. Zhang et al. 2018; Lim et al. 2020). However, most of these techniques have several drawbacks including high costs, complicated processes, and poor selectivity, which make their application rather questionable. Adsorption technique, as the most attractive and competitive

Responsible Editor: Philippe Garrigues

✉ Mahdi Hasanzadeh
m.hasanzadeh@yazd.ac.ir

Hossein Shahriyari Far
h_shahriyarifar@alumni.iust.ac.ir

Mohammad Shabani Nashtaei
shabani_m@alumni.iust.ac.ir

Mahboubeh Rabbani
m_rabani@iust.ac.ir

[1] Department of Chemistry, Iran University of Science and Technology, Narmak, P.O. Box 16846-13114, Tehran, Iran

[2] Department of Textile Engineering, Yazd University, P.O. Box 89195-741, Yazd, Iran

approach, is a cost-effective, simple operation, highly efficient, and reliable approach (Molavi et al. 2018; El Salam and Zaki 2018; Kousha et al. 2012; Qiu et al. 2017; Hasanzadeh et al. 2019; Khan et al. 2019). Various adsorbents such as activated carbon (Di Natale et al. 2017), graphene (J. Li et al. 2019), biopolymers (Mincke et al. 2019; Elwakeel et al. 2021; Elwakeel et al. 2013; El-Shorbagy et al. 2021), magnetic composites (Donia et al. 2007), and nanofibers (Moawed et al. 2016) have been developed to efficiently recover the precious metals from dilute solutions.

Metal–organic frameworks (MOFs), as an emerging nanoporous crystalline material with fascinating physicochemical features, have widely been considered for the adsorption process. They exhibit high porosity, tunable pore size, large specific surface area, and high thermal and chemical stability, which make them potentially suitable for many applications (Khiarak et al. 2020; Moghadam et al. 2020), especially for wastewater treatment (Hasanzadeh et al. 2020; Hasanzadeh et al. 2019) and precious metal recovery (Khiarak et al. 2020; Lin et al. 2018). Studies have shown the recovery of Pd(II) from acidic solution using MOFs with different structures (Lin et al. 2019). Incorporation of nanomaterials such as magnetic nanoparticles to MOF structures has shown further improvement and rapid extraction of adsorbent on wastewater treatment and metal recovery (Zhao et al. 2015; Abdi et al. 2019; Hamedi et al. 2019). For instance, magnetic copper-based MOF was successfully applied for the adsorption of palladium from different environmental samples (Bagheri et al. 2012).

The surface modification and functionalization of magnetic MOFs (MMOFs) are suggested which could provide more potential adsorbents with active functional groups to improve the adsorption efficiency (X. Zhang et al. 2020). Several approaches have been made for modification of MMOFs, such as mercaptoacetic acid (Huang et al. 2016), poly(4-vinylpyridine) (Li et al. 2020a, b), glutathione (Liu et al. 2018), and cetrimonium bromide (CTAB) (Li et al. 2020a, b). In a recent study, magnetic MOF composite was modified with β-cyclodextrin to enhance the adsorption selectivity toward triazole fungicides (Senosy et al. 2020). Dendrimers, as highly branched three-dimensional structures, possess a large number of functional end groups which make them appealing for adsorption-based applications. In recent years, great attention has been paid to the dendrimer modification of common adsorbents for metal uptake (Yen et al. 2017; Krawczyk et al. 2016; Kanani-Jazi et al. 2020) and wastewater treatment (Hayati et al. 2015; Yang et al. 2019).

In this work, we studied the post-modification of magnetic zirconium-based MOF nanocomposite with second-generation poly(propyleneimine) (PPI) dendrimer for removal of Pd(II) ions from aqueous solution. We have hypothesized that the unique characteristics of highly stable nanoporous zirconium-based MOF, as well as highly functional branched dendrimer, could contribute to an efficient and sustainable precious metal recovery. The magnetic property of Fe_3O_4 nanoparticles also offers a simple and effective way for the regeneration of adsorbents and recovery of metal ions. To our knowledge, there is no report on literature dealing with the adsorption of metal ions on such hybrid dendritic magnetic nanostructures. The Pd(II) uptake on dendrimer-modified MMOF (MMOF@PPI) was studied. The effects of four parameters including adsorbent content, Pd ion concentration, solution pH, and contact time were investigated through response surface methodology (RSM). Investigation of Pd(II) uptake capacity of MMOF@PPI was conducted through adsorption kinetics and isotherms models.

Experiments

Materials

Zirconium chloride ($ZrCl_4$, purity ≥ 98%), terephthalic acid (purity ≥ 98%), *N*,*N*-dimethylformamide (DMF), acetic acid (HAc), ammonia (25%), palladium standard solution (1 g/L), thiourea, hydrochloric acid, ethanol, and methanol were received from Merck Co. (Germany). Iron chloride hexahydrate ($FeCl_3{\cdot}6H_2O$, purity ≥ 99%) and iron chloride tetrahydrate ($FeCl_2{\cdot}4H_2O$, purity ≥ 99%) were obtained from Sigma-Aldrich (USA). Second-generation PPI dendrimer was also purchased from SyMO-Chem (Netherlands). All the chemicals were analytical grade and were used without further purification.

Synthesis of magnetic MOF (MMOF)

MMOF adsorbent was synthesized according to the reported procedure (Far et al. 2020). First, Fe_3O_4 particles in spherical morphology were prepared by the coprecipitation method (Huang et al. 2015). Briefly, $FeCl_3{\cdot}6H_2O$ and $FeCl_2{\cdot}4H_2O$ in a 2:1 ratio were mixed with water under a nitrogen atmosphere. After stirring at 80°C for 3 h, 25% ammonia was added and stirring continued at the same temperature for 5 h. The product was magnetically separated and washed with water and dried at 70°C for 24 h. Then the MMOF material was synthesized solvothermally on as-prepared Fe_3O_4 particles. At first, a mixture of $ZrCl_4$ (0.15 g), terephthalic acid (0.13 g), DMF (80 mL), acetic acid (4 mL), and newly synthesized Fe_3O_4 particles (0.2 g) was prepared (Wu et al. 2018). The mixture was transferred into a Teflon autoclave followed by solvothermal treatment at 130°C for 12 h. After the autoclave cooled down to room temperature, the product was washed three times with water and ethanol. Finally, the brown MMOF particles were obtained by drying at 80°C for 12 h.

Modification of MMOF with dendrimer (MMOF@PPI)

The MMOF particles (200 mg) were added to the dendrimer solution (200 μL) and then it was stirred for 2 h at room temperature. The modified MMOF particles (MMOF@PPI) were separated using an external magnet, washed with methanol and ethanol, and then dried at 40°C overnight. Scheme 1 shows the schematic representation of the MMOF@PPI synthesis procedure.

Characterizations

Fourier transform infrared (FTIR) spectra of MMOF adsorbents were measured on Avatar FTIR spectrophotometer (Thermo Nicolet, USA). The crystalline structure of synthesized MMOF adsorbents was obtained using powder X-ray diffraction (PXRD) (Philips, Expert Pro, Netherlands) with Cu Kα radiation. The vibrating sample magnetometer (Meghnatis Daghigh Kavir Co., Iran) was also used to measure the magnetic properties of the MMOF adsorbents. The morphology and size of synthesized MMOF adsorbents were studied through field emission scanning electron microscopy (FESEM, TESCAN, Mira 3, Czech Republic). The N_2 adsorption/desorption isotherms of synthesized adsorbents were determined at 77 K using the BELSORP-MINI II instrument (BEL Japan, Inc.). The zeta potential of the dendrimer-modified MMOF in deionized water was measured by the WALLIS zeta potential analyzer (Cordouan Technologies). The concentration of Pd ion before and after adsorption was determined using ICP optical emission spectrometer (Shimadzu, ICP-7000 ver. II).

Adsorption experiments

The absorption experiments were performed at 25°C using palladium solutions with MMOF and MMOF@PPI adsorbents. The effect of processing conditions (MMOF content, Pd ion concentration, contact time, and pH) on the adsorption efficiency was investigated. Aqueous solutions of Pd ion with different concentrations (20–100 ppm) were prepared in deionized (DI) water. A specific amount (10–20 mg) of MMOF adsorbent was added into 50 mL of Pd aqueous solution and shaken using an orbital shaker (Heidolph Unimax 1010, Germany) at 400 rpm. The pH of each solution was adjusted on different values in the range of 2–7 using HCl (0.01 M) and NaOH (0.01 M). At certain time intervals (5–150 min), the MMOF adsorbent was separated magnetically using an external strong magnet. Finally, the Pd ion concentration was determined with the ICP-OES instrument. The Pd uptake (q_t) on the MMOFs at a given time (t) is calculated based on the following equation (Iqbal et al. 2016):

$$q_t(mg/g) = \frac{V(C_0 - C_t)}{m} \quad (1)$$

where V (L) is the volume of the Pd solution, m (g) is the mass of MMOF adsorbent, and C_0 and C_t (mg/L) are the Pd ion concentration at $t = 0$ and t, respectively.

Regeneration study

The reusability of MMOFs as an important characteristic of adsorbents was investigated according to the procedure reported in the literature (Lin et al. 2019). The Pd ion was completely eluted from Pd-loaded MMOF and MMOF@PPI

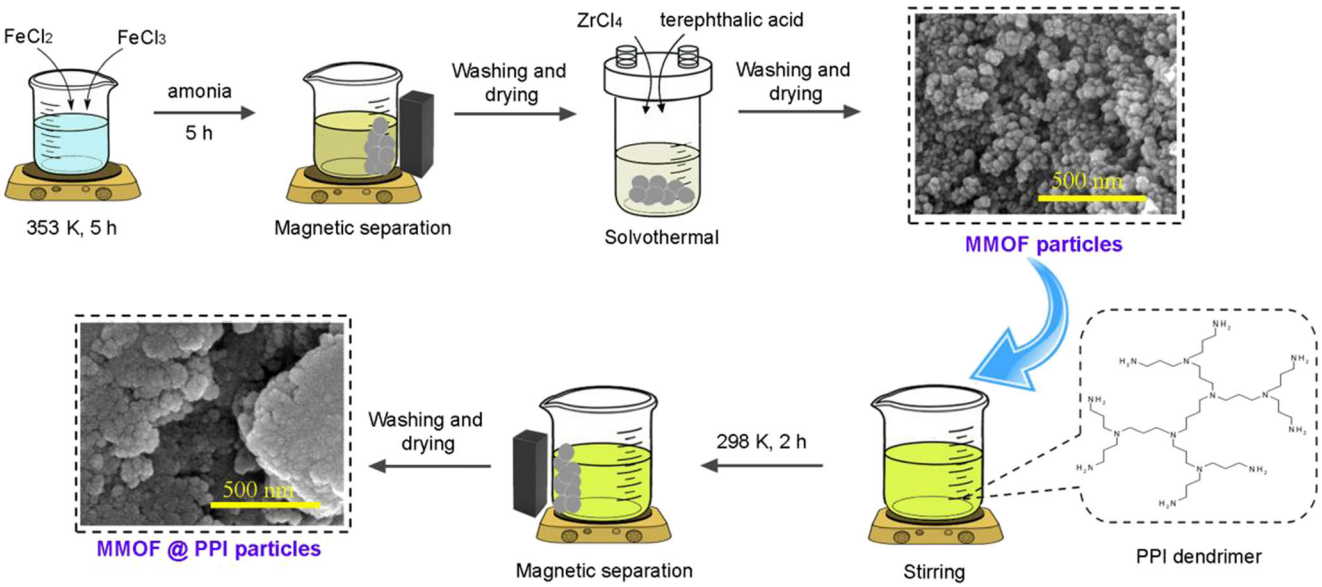

Scheme 1 Schematic illustration showing the synthesis and dendrimer modification of MMOF

adsorbents at pH 1.0 for 24 h, followed by rinsing three times with 10 mL of acidified thiourea. Then it was rinsed twice with 20 mL of HCl (0.1 M) and distilled water. Such adsorption–desorption cycles were repeated twice.

Experimental design

The effect of adsorption process conditions on metal uptakes, a statistical approach based on response surface methodology (RSM), was carried out. Affecting parameters, including MMOF@PPI content (mg), Pd ion concentration (ppm), and contact time (min), were considered as independent variables, and Pd uptake (mg/g) was a dependent variable (response). The central composite design (CCD) consisting five levels (coded as −alpha, −1, 0, +1, and +alpha) was utilized (Table S1). The small CCD design matrix with corresponding results of Pd uptakes on MMOF@PPI adsorbent is tabulated in Table S2. The predicted response (Pd uptakes, Y) was expressed by the following second-order polynomial equation:

$$Y = \alpha_0 + \sum_{i=1}^{n} \alpha_i X_i + \sum_{i=1}^{n} \alpha_{ii} X_i^2 + \sum_{i=1}^{n-1} \sum_{j=2}^{n} \alpha_{ij} X_i X_j + \varepsilon \qquad (2)$$

Where X_i and X_j were coded values of independent variables. α_0, α_i, α_{ii}, and α_{ij} were also regression coefficients for the constant, linear, quadratic, and interaction effects, respectively (Myers et al. 2009).

Results and discussion

Structural characterization

PXRD patterns of MOF and MMOF were obtained to study their crystalline structure (Fig. 1a). It can be seen that the MMOF particles exhibit the main diffraction peaks of MOF (2θ = 7.4, 8.6, and 25.7°) and Fe_3O_4. It indicated that the crystalline MOF was successfully grown onto the Fe_3O_4 surface. The successful modification of MMOF with PPI dendrimer was followed by FTIR spectroscopy of MMOF and MMOF@PPI (Fig. 1b). The characteristic peak of Zr-based MOF is visible in the FTIR spectrum of MMOF (Hasanzadeh et al. 2019). The peaks at 746 and 660 cm^{-1} illustrated the Zr-O vibration of Zr-based MOF. The adsorptions of carboxyl groups on the terephthalic acid ligands appeared at 1395, 1585, and 1658 cm^{-1} (Huo et al. 2019). In the spectrum of MMOF@PPI, the extra adsorption (around 1022 cm^{-1}) belonged to the CN stretching vibration of the PPI dendrimer. Moreover, the increased adsorption band around 3440 cm^{-1} is attributed to both O-H stretching vibration of adsorbed water and the N-H stretching of PPI dendrimer primary amine groups (Kayal and Chakraborty 2018). Therefore, the MMOF particles were successfully modified with PPI dendrimer.

The nitrogen adsorption/desorption isotherm of MMOF and MMOF@PPI adsorbents was obtained to analyze their specific surface area and pore volume (Fig. 1c). They showed a hybrid I/II mixed type isotherm at 77 K with H_4 hysteresis loop, consistent with previous literature (Chen et al. 2019a, b; Huo et al. 2019). The obtained results exhibit the high BET surface area of 507 m^2/g for MMOF particles rather than Fe_3O_4 particles (about 11 m^2/g), which is beneficial for the adsorption of metal ions. The pore volume of MMOF adsorbent was also increased to 0.58 cm^3/g, suggesting successful synthesis of high specific surface area MOFs on magnetic particles. The BET surface area of MMOF@PPI (120 m^2/g) was rationally expected to slightly decrease due to the surface modification of MMOF with dendrimer and surface coverage of the particles. Although the modification of MMOF with dendrimer leads to a reduction in the surface area, the provided large number of functional ending groups could contribute to efficient adsorption. Pore size distribution analysis of MMOF and MMOF@PPI (Fig. 1d) indicated the micromesoporous characteristics of magnetic adsorbents, which facilitate the diffusion of metal ions to accessible active sites within the pores.

Magnetic properties of the MMOF adsorbents were further studied. The magnetic hysteresis loops of MMOF and MMOF@PPI particles (Figure S1) revealed the relatively soft ferromagnetic behavior of magnetic adsorbents. Compared to that of MMOFs, higher saturation magnetization and coercivity were obtained for MMOF@PPI. The morphology of MMOF adsorbents was observed by FESEM. Figure 2 has confirmed the regular morphology with the semispherical shape of MMOF particles. The particle size of MMOF is in the range of 20–50 nm. Modification of MMOF with dendrimer leads to the formation of aggregated irregular microspheres.

Statistical analysis and model validation

The second-order polynomial equation was developed to correlate the Pd uptakes (Y) as the function of MMOF@PPI content (X_1), Pd ion concentration (X_2), and contact time (X_3) by using the analysis of variance (ANOVA). The confidence level was selected to be 95%, which means the model terms will be significant if their probability value is smaller than 0.05. The results of ANOVA (Table S3) confirmed that the model is highly significant. Furthermore, it was concluded that the terms X_1X_3, X_2X_3, X_2^2, and X_3^2 have no significant effect on Pd uptake at the studied confidence level.

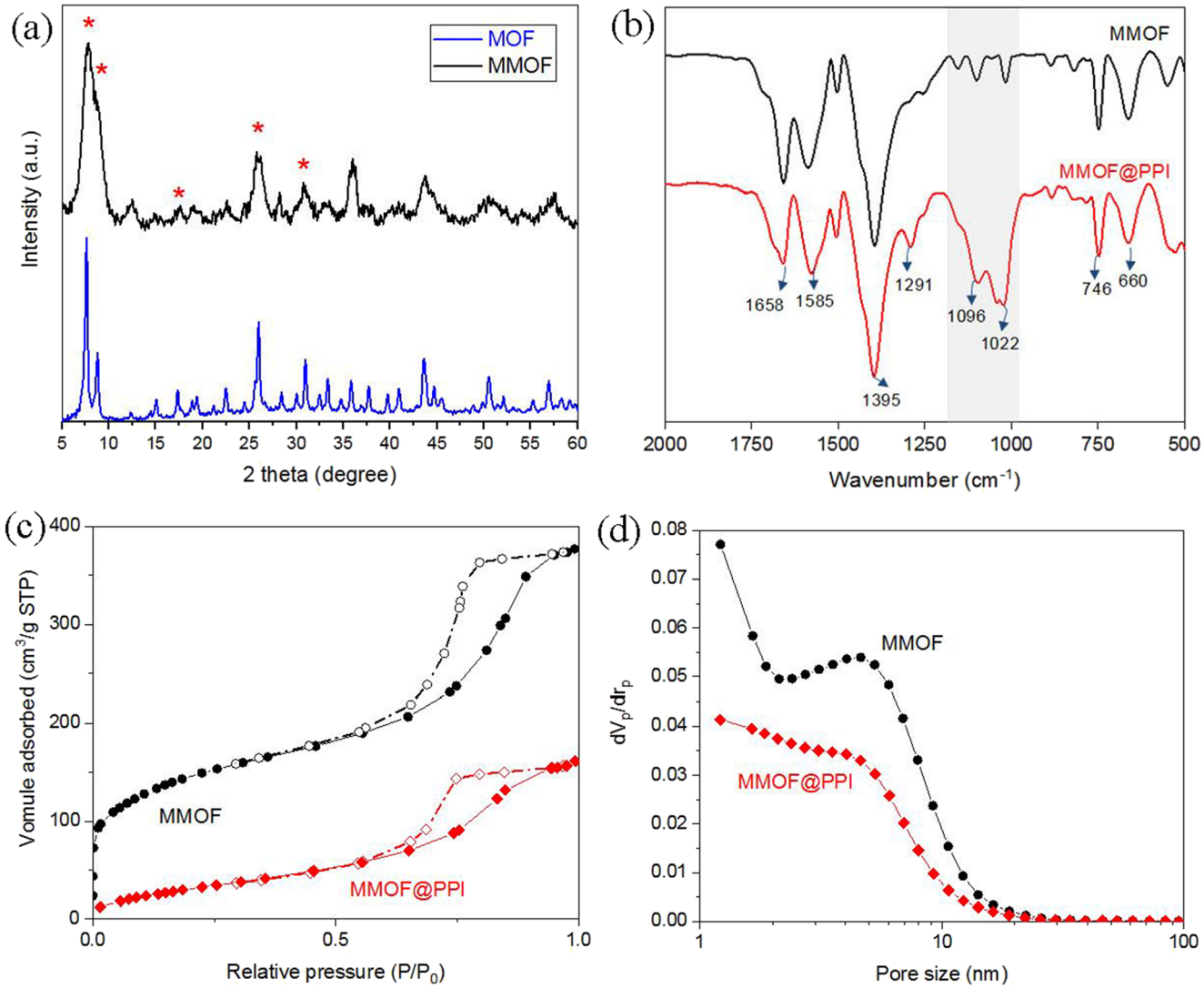

Fig. 1 Characteristics of magnetic adsorbents. **a** XRD patterns of MMOF (the main diffraction peaks of MOF are marked as "*"), **b** FTIR spectrum, **c** nitrogen adsorption/desorption isotherm, and **d** BJH pore size distribution of MMOF and MMOF@PPI adsorbents

Therefore, the final fitted regression equation in a coded unit is obtained as follows:

$$R(\%) = +146.16 - 24.88X_1 + 44.45X_2 - 1.50X_3 - 12.35X_1X_2 + 6.27X_1^2 \quad (3)$$

where X_1, X_2, and X_3 represent the MMOF@PPI content, Pd ion concentration, and contact time, respectively. The coefficient of determination (R^2) and adjusted R^2 (R^2_{adj}) are 0.984 and 0.975, respectively, advocating a close agreement

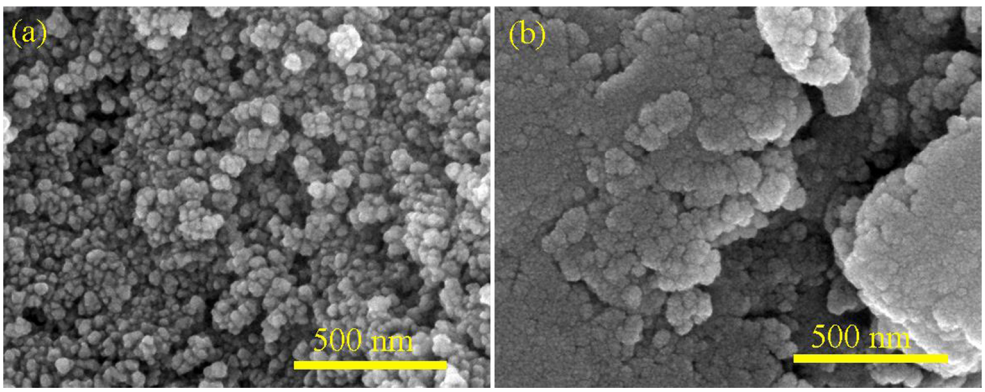

Fig. 2 FESEM micrographs of **a** MMOF and **b** MMOF@PPI materials

between the model predicted data and the experiments (Figure S2). The high adequate precision of 36.32 (the value above 4) confirms adequate model discrimination. The obtained results suggested that the model was satisfactorily capable of predicting the Pd uptakes on dendrimer-modified MMOF adsorbents.

Figure 3 represents the 3D response surface and contour plot of the Pd uptakes as the function of MMOF@PPI content (mg) and Pd ion concentration (ppm) in the constant contact time of 50 min. It was found that as the amount of MMOF@PPI increased, the Pd uptake decreased. This reduction intensified at a higher level of MMOF@PPI content. This could be ascribed to the splitting effect of flux between the Pd ion concentrations and the dendrimer-modified MMOF surface. Increasing the MMOF@PPI content causes a decrease in the amount of Pd metal ions adsorbed onto the unit weight of MMOF@PPI. This could also be responsible for increasing metal uptakes observed with increasing initial Pd concentration.

The optimum conditions for efficient Pd uptakes were obtained based on the RSM model. The variables were set in their investigated range. The maximum Pd uptakes were predicted to be 235.6 mg/g at MMOF@PPI content of 12.5 mg, Pd ion concentration of 80 ppm, and contact time of 40 min. Further experiment at the optimal conditions was carried out to confirm the predictivity of the regression model. An uptake of 234 mg/g was obtained, demonstrating close agreement with predicted Pd uptake.

Adsorption kinetics

The effect of contact time on Pd uptake on MMOF and MMOF@PPI materials was assessed (Fig. 4). Figure 4a shows that the adsorption capacity of Pd ions increased rapidly in 80 min and gradually reached equilibrium at 150 min. A fast and efficient Pd ion uptake on both magnetic adsorbents was carried out in the first minutes. The Pd adsorption rate of dendrimer-modified MMOF was found to be faster than the unmodified one. The Pd uptake on both magnetic adsorbents exhibits a fast initial Pd uptake followed by slow adsorption until the equilibrium is reached. The equilibrium Pd uptake (q_e) on MMOF and MMOF@PPI was found to be about 204 and 291 mg/g, respectively.

Three kinetic models including intraparticle diffusion (IPD), pseudo-first-order (PFO), and pseudo-second-order (PSO) models were utilized to describe the kinetics of Pd uptake on magnetic adsorbents by considering the following equations (Oladipo et al. 2014; Embaby et al. 2018):

$$q_t = K_P t^{0.5} + I \tag{4}$$

$$\ln(q_e - q_t) = \ln q_e - k_1 t \tag{5}$$

$$\frac{t}{q_t} = \frac{1}{k_2 q_e^2} + \frac{t}{q_e} \tag{6}$$

where K_P (mg/g·min$^{0.5}$) is the rate constant of interparticle diffusion and I is the intercept representing the thickness of the boundary layer. q_e and q_t are the Pd uptakes at equilibrium and at a time t, respectively. k_1 (1/min) and k_2 (g/mg.min) are also the rate constants of PFO and PSO models, respectively (Ayub et al. 2019; Sharifi et al. 2019). The linear plots of kinetic models are shown in Fig. 4. Table 1 summarizes the calculated adsorption kinetic parameters for all models. The obtained results indicate that the Pd uptake on both magnetic adsorbents best abides the pseudo-first-order model. This result confirms that the physisorption could be considered as the main driving force of Pd(II) uptake on magnetic adsorbents (Dragan and Loghin 2013), consisting of the results obtained from adsorption isotherm. The value of the rate constant of MMOF@PPI was found to be higher than MMOF adsorbent, revealing the faster kinetics of Pd uptake on dendrimer functionalized materials. This may be ascribed to the synergistic

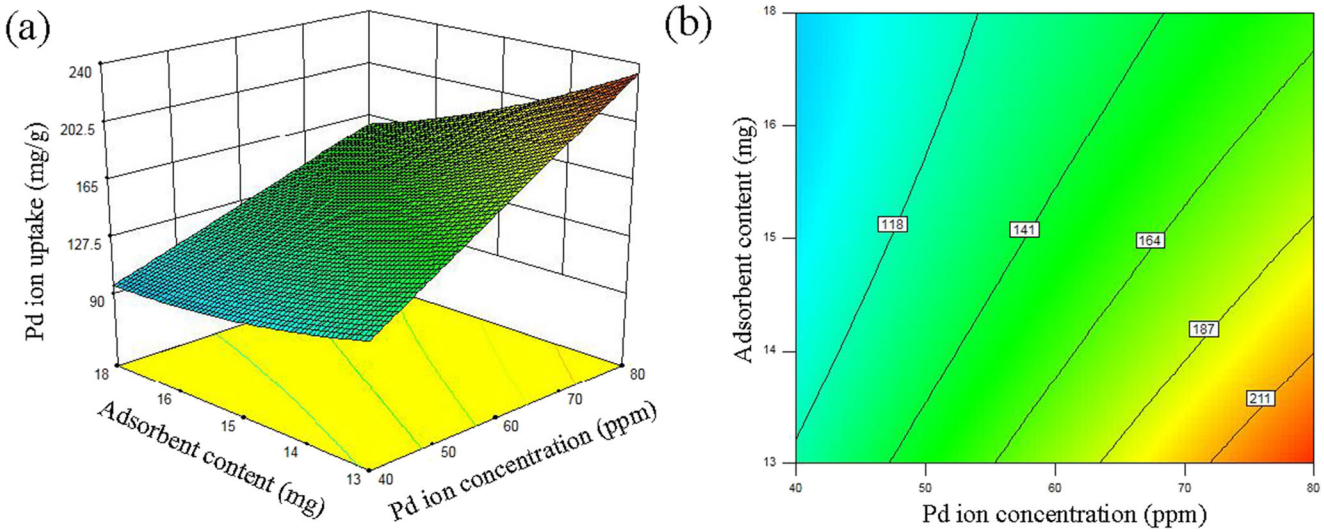

Fig. 3 **a** A 3D response surface and **b** contour plots showing the effect of MMOF@PPI content and Pd ion concentration on the Pd uptakes

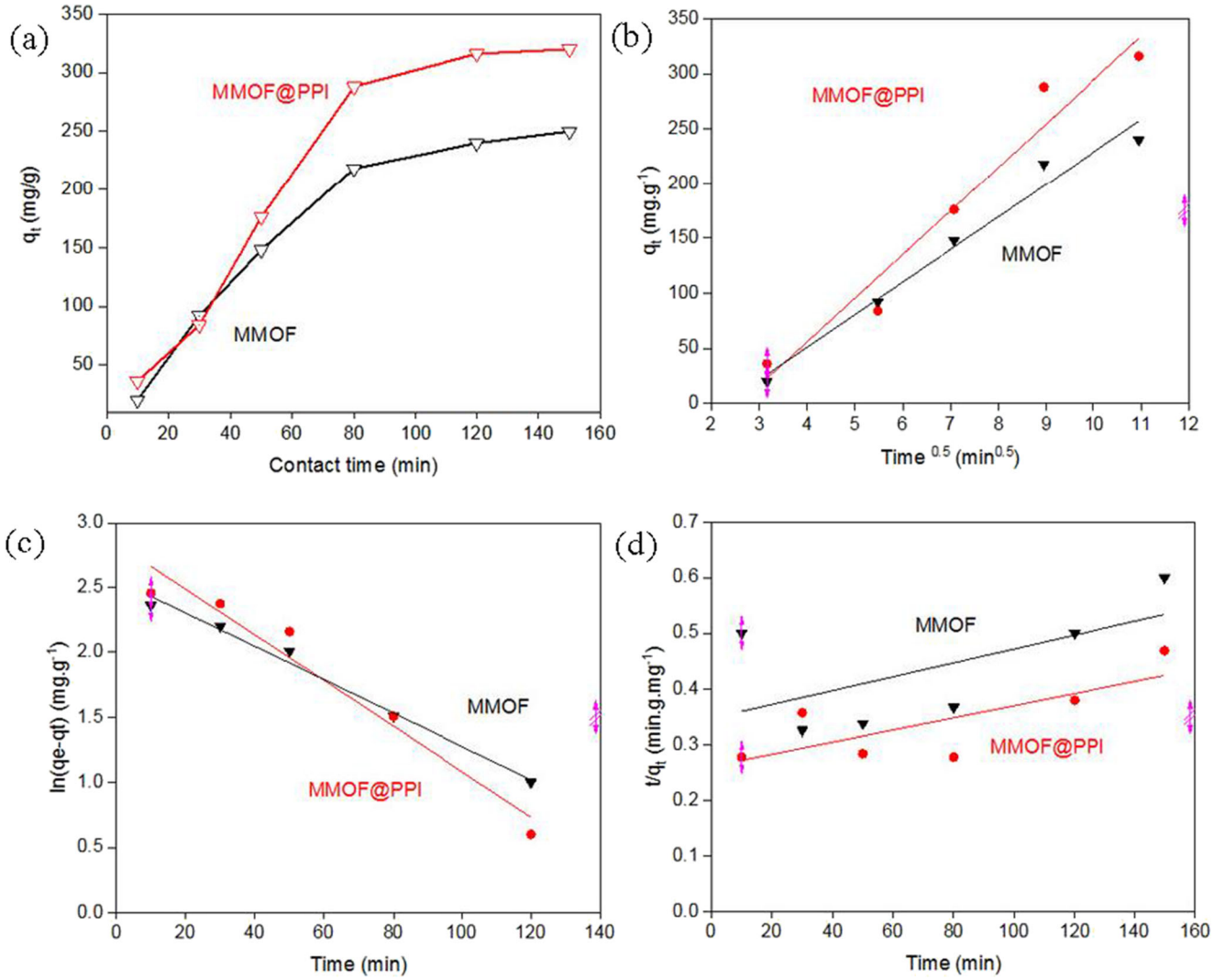

Fig. 4 **a** Effect of contact time on Pd uptake, **b** intraparticle diffusion model, **c** pseudo-first-order model, and **d** pseudo-second-order model for adsorption of Pd ions on MMOF and MMOF@PPI (pH = 4, the content of magnetic adsorbents = 12.5 mg, Pd ion concentration = 80 ppm)

effect of the nanoporous structure of MMOF particles and a large number of functional groups on the dendrimer surface.

Effect of pH

In this study, the effect of pH has been evaluated in the range of 2–7 to optimize the pH value for maximum Pd(II) uptake. Figure 5a shows the effect of pH on Pd(II) uptake on MMOF and MMOF@PPI adsorbents. It is obvious that the Pd(II) uptake on both magnetic adsorbents is strongly affected by pH value. It indicates that the maximum uptake (204 and 291 mg/g for MMOF and MMOF@PPI, respectively) has occurred at pH near 4. Dendrimer-modified MMOF exhibits higher Pd(II) uptake throughout all pH values rather than MMOF, which could be

Table 1 Kinetic model parameters of Pd uptake on magnetic adsorbents (pH = 4, the content of magnetic adsorbents = 12.5 mg, Pd ion concentration = 80 ppm)

Magnetic adsorbent	$(q_e)_{Exp.}$ (mg/g)	Intraparticle diffusion model			Pseudo-first-order model			Pseudo-second-order model		
		K_P (mg/g.min$^{0.5}$)	I	R^2	$(q_e)_{Cal.}$ (mg/g)	k_1 (1/min)	R^2	$(q_e)_{Cal.}$ (mg/g)	k_2 (g/mg.min)	R^2
MMOF	204	29.65	67.5	0.976	354	0.029	0.988	833	0.00004	0.366
MMOF@PPI	291	39.74	103	0.956	676	0.04	0.955	902	0.00004	0.587

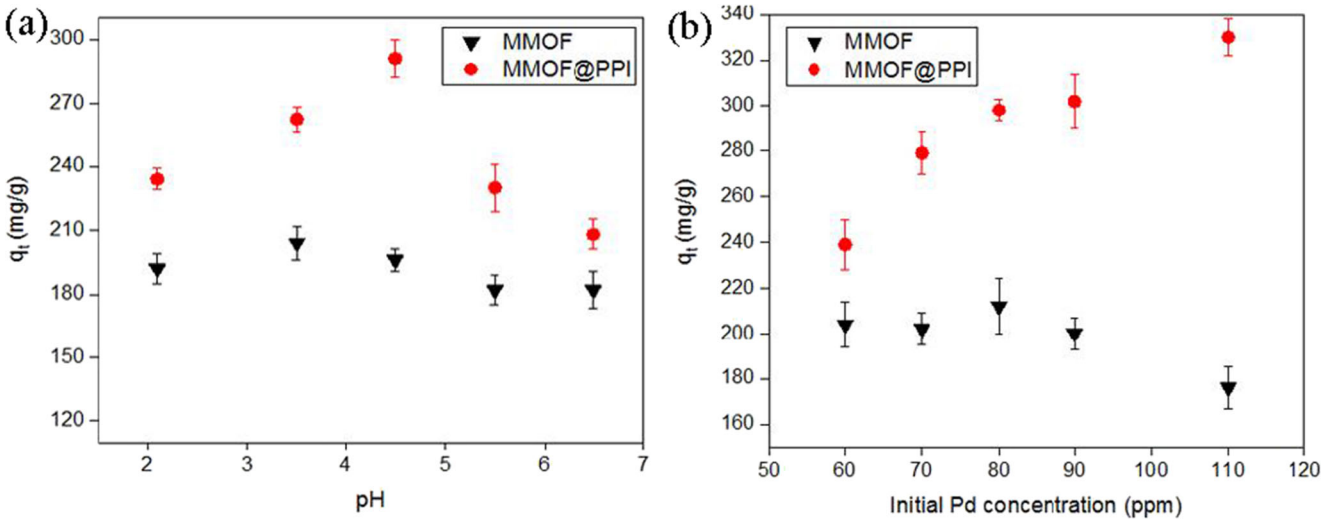

Fig. 5 Effect of **a** pH and **b** initial Pd ion concentration on Pd uptakes on MMOF and MMOF@PPI (the content of magnetic adsorbents = 12.5 mg, contact time = 40 min)

ascribed to the high binding affinity of PPI dendrimers toward metal ions (Yen et al. 2017). Moreover, the cationic zirconium nodes in MOF (UiO-66) are considered as further binding sites for Pd(II) ions (Lin et al. 2018). The zeta potential measurement indicated that the MMOF@PPI is positively charged at neutral pH value (~6.5) and low pH and thus capable of forming electrostatic adsorption. It is well-known that at low pH, the surface of the adsorbent would be protonated and gives positive zeta potential.

Adsorption isotherms

The effect of initial Pd ion concentration, as one of the most important data for understanding the mechanism of adsorption, was investigated in the range of 60 to 110 ppm. As shown in Fig. 5b, the dendrimer-modified MMOF has a higher Pd uptake capacity than the unmodified one with maximum uptake of 330 mg/g at an initial Pd concentration of 110 ppm. A large number of functional end groups on the surface of dendrimer-modified MMOF particles could be responsible for this increase in Pd uptake. Further investigations on the mechanism of Pd uptake were carried out using Langmuir, Freundlich, and Tempkin isotherm models. The Langmuir isotherm model assumes monolayer sorption onto specific homogeneous sites, while the Freundlich isotherm model describes the heterogeneous adsorption process (Mohammad et al. 2011; Liu et al. 2016). The linear forms of Langmuir, Freundlich, and Tempkin isotherm models are expressed by the following equations (Liu et al. 2016):

$$\frac{C_e}{q_e} = \frac{1}{K_L q_{\max}} + \frac{C_e}{q_{\max}} \tag{7}$$

$$\ln q_e = \ln K_F + \frac{1}{n}\ln C_e \tag{8}$$

$$q_e = B\ln K_T + B\ln C_e \tag{9}$$

where C_e (mg/L) is the Pd ion concentration at equilibrium. K_L (L/mg) and K_F ((mg/g)(L/mg)$^{1/nF}$) are the Langmuir and Freundlich constants, respectively. The term $1/n$ is related to the adsorption intensity (Heydari Moghaddam et al. 2019; Baziar et al. 2021). B (J/mol) and K_T (L/mg) are also the Tempkin constants.

Figure S3 shows the linear plots of Langmuir, Freundlich, and Tempkin isotherms for Pd uptake on MMOF and MMOF@PPI adsorbents. Considering the linear isotherm constants (Table 2) revealed that the uptake of Pd ions on both magnetic adsorbents was well matched by the Langmuir isotherm model. It implies that the Pd ions were adsorbed homogeneously on a monolayer surface of magnetic adsorbents.

Adsorption thermodynamics

The adsorption thermodynamic was investigated at different temperatures in the range of 298–318 K under the optimum conditions. The thermodynamic parameters of Pd uptake on MMOF and MMOF@PPI materials are given in Table 3. Thermodynamic parameters including Gibbs free energy (ΔG^0), enthalpy (ΔH^0), and entropy (ΔS^0) were calculated by the following equations (Lima et al. 2019; Y. Liu and Liu 2008; W. Zhang et al. 2019):

$$\Delta G^0 = \Delta H^0 - T\Delta S^0 \tag{10}$$

$$\ln\left(\frac{q_e}{C_e}\right) = \frac{\Delta S^0}{R} - \frac{\Delta H^0}{RT} \tag{11}$$

where R (8.314 J/mol.K) and T (K) are the universal gas constant and the temperature of the solution, respectively. The ΔG^0 value decreased with increasing temperature from 298 to 318 K for both MMOF and MMOF@PPI materials. The

Table 2 Linear isotherm constants for Pd uptake on magnetic adsorbents (pH = 4, the content of magnetic adsorbents = 12.5 mg, contact time = 40 min)

Magnetic adsorbent	Langmuir			Freundlich			Tempkin		
	K_L (L/mg)	q_{max} (mg/g)	R^2	n	K_F ((mg/g)(L/mg)$^{1/nF}$)	R^2	B (kJ/mol)	K_T (L/mg)	R^2
MMOF	0.06	152	0.967	16.12	239.8	0.437	0.21	54.79	0.39
MMOF@PPI	0.01	555	0.951	28.9	281	0.967	0.25	3.34	0.78

negative value of ΔG^0 indicated that the adsorption of Pd on both magnetic adsorbents is spontaneous. Moreover, the positive values of ΔH^0 confirm the endothermic nature of the adsorption.

Regeneration and reusability of adsorbents

The regeneration and the potential reusability of an adsorbent are additional features for the commercialization of the product. Cycles of the adsorption–desorption process were conducted, and the result was shown in Figure S4. The results showed that the adsorption capacity of both magnetic adsorbents was slightly decreased, as the number of adsorption–desorption cycles was increased. However, this reduction was lower for the dendrimer-modified adsorbent. The MMOF@PPI retained 92% of its capacity after two cycles of adsorption–desorption, while this value was found about 85% for unmodified MMOF. The results confirmed the reversibility of adsorption sites on dendrimer-modified adsorbent. Further investigation on the structural stability of magnetic adsorbent in water and acidic environments (HCl 0.1 M) for 7 days at 25°C (Figure S5) has shown their good stability and potential practical applicability in harsh environments.

Comparison with other adsorbents

Table 4 summarizes the comparison between the Pd(II) uptake capacity of MMOF@PPI and other reported adsorbents. The data indicate that the dendrimer-modified MMOF exhibits fast and efficient adsorption of Pd(II) compared to other materials. MMOF@PPI also provides easy separation of Pd, thanks to its good magnetic properties. The high adsorption capacity of MMOF@PPI, which is benefited from a high specific surface area and a large number of functional groups, makes it an outstanding material for the recovery of precious metals and wastewater treatment.

Conclusions

A novel magnetic adsorbent (MMOF@PPI) was successfully synthesized and utilized for adsorption and recovery of Pd(II) from an aqueous solution. The most important findings are summarized as follows:

- The prepared dendrimer-modified adsorbent possessed a superior figure of merits as compared to the unmodified one, such as high magnetic properties and a large number of active sites for Pd(II) uptake.
- The Pd(II) uptake on dendrimer-modified magnetic adsorbent was described by the pseudo-first-order kinetic model.
- The adsorption isotherm of dendrimer-modified magnetic adsorbent was fitted to the Langmuir isotherm model, suggesting homogeneous adsorption on a monolayer surface of adsorbents.
- The Pd adsorption capacity of dendrimer-modified MMOF was 43% higher than the MMOF.
- Investigating the impact of adsorption parameters through RSM revealed that the maximum metal uptake (291 mg/g) will be achieved at optimal conditions of 12.5 mg adsorbent content, 80 ppm Pd concentration, pH = 4, and contact time of 40 min.

Table 3 Thermodynamic parameters for adsorption of Pd ions on magnetic adsorbents (the content of magnetic adsorbents = 12.5 mg, Pd ion concentration = 80 ppm, contact time = 40 min, pH = 4)

Magnetic adsorbent	Temperature (K)	Thermodynamic parameters		
		ΔG^0 (kJ/mol)	ΔH^0 (kJ/mol)	ΔS^0 (J/mol.K)
MMOF	298	−5/10	7.06	0.04
	308	−5/35		
	318	−5/89		
MMOF@PPI	298	−9/88	53.2	0.2
	308	−11/08		
	318	−13/93		

Table 4 Summary of various adsorbents for Pd(II) uptake

Adsorbent	Adsorption conditions				Pd(II) uptake (mg/g)	Ref.
	pH	t (h)	C_0 (ppm)	m (mg)		
Graphene oxide (GO)	5	16	60	2	98.32	L. Liu et al. (2012)
Glutaraldehyde crosslinked chitosan	3	16	65	2	180.18	L. Liu et al. (2012)
Chitosan/GO	3	16	65	2	216.92	L. Liu et al. (2012)
UiO-66	4.5	5	1.5	10	125.0	Daliran et al. (2020)
UiO-66-NH2	4.5	5	1.5	10	197.0	Daliran et al. (2020)
Pyridyltriazol-functionalized UiO-66	4.5	5 min	1.5	10	294.1	Daliran et al. (2020)
Polyethyleneimine-functionalized alumina nanopowder	6	9 min	10	100	97.7	Nagarjuna et al. (2017)
Dendrimer-modified magnetic nanoparticles	6.5	8	20	--	2.71	Yen et al. (2017)
Ethylenediamine-lignin	--	24	0.186 mM	20	22.66	Parajuli et al. (2006)
Aliquat-336 impregnated mesoporous silica	4	3	40	50	212.76	Sharma et al. (2016)
MOF-802	1	8	100	10	25.8	Lin et al. (2019)
UiO-66	1	1	1600	10	105.1	Lin et al. (2019)
MOF-808	1	1	1600	10	163.9	Lin et al. (2019)
MIL-101(Cr)-NH_2	1	24	87.6	10	277.6	Lim et al. (2020)
MIL-101(Cr)-NO_2	1	24	87.6	10	119.5	Lim et al. (2020)
Poly(4-vinylpyridine)-grafted rGO	2	6	100	200	177.0	Chen et al. (2019a, b)
Glycine modified crosslinked chitosan	2	2	50	100	120.39	Ramesh et al. (2008)
Thiourea-modified chitosan	2	4	80	100	112.36	Zhou et al. (2009)
Ethylenediamine-modified magnetic chitosan nanoparticles	2	1	60	50	138.0	Zhou et al. (2010)
Persimmon powder-formaldehyde resin	1	24	680	--	259.7	Yi et al. (2016)
Rubeanic acid derivative chitosan	2	72	80	--	352.0	Guibal et al. (2002)
MMOF	4	40 min	80	12.5	204	This study
MMOF@PPI	4	40 min	80	12.5	291	This study

Note: –, not mentioned in the reference

- The results of this research demonstrate that the MMOF@PPI adsorbent is not only suitable for metal ion adsorption, but also can be used for other applications such as wastewater treatment.

Supplementary Information The online version contains supplementary material available at https://doi.org/10.1007/s11356-021-15144-2.

Availability of data and materials Not applicable.

Author contribution Hossein Shahriyari Far: investigation, methodology, visualization, and writing: original draft. Mahdi Hasanzadeh: conceptualization, supervision, resources, formal analysis, funding acquisition, project administration, and writing — review and editing. Mohammad Shabani Nashtaei: investigation, methodology, and visualization. Mahboubeh Rabbani: conceptualization, supervision, resources, formal analysis, and validation.

Funding MH thanks the Iran National Elites Foundation (INEF, Grant No. 15-89661) for the financial support.

Declarations

Ethical approval Not applicable.

Consent to participate Not applicable.

Consent forpublication Not applicable.

Competing interests The authors declare no competing interests.

References

Abdi J, Mahmoodi NM, Vossoughi M, Alemzadeh I (2019) Synthesis of magnetic metal-organic framework nanocomposite (ZIF-8@SiO2@MnFe2O4) as a novel adsorbent for selective dye removal from multicomponent systems. Microporous Mesoporous Mater 273:177–188. https://doi.org/10.1016/j.micromeso.2018.06.040

Ayub S, Mohammadi AA, Yousefi M, Changani F (2019) Performance evaluation of agro-based adsorbents for the removal of cadmium from wastewater. Desalin Water Treat 142:293–299. https://doi.org/10.5004/dwt.2019.23455

Bagheri A, Taghizadeh M, Behbahani M, Asgharinezhad AA, Salarian M, Dehghani A, Ebrahimzadeh H, Amini MM (2012) Synthesis and characterization of magnetic metal-organic framework (MOF) as a novel sorbent, and its optimization by experimental design methodology for determination of palladium in environmental samples. Talanta 99:132–139. https://doi.org/10.1016/j.talanta.2012.05.030

Baziar M, Zakeri HR, Ghalehaskar S, Nejad ZD, Shams M, Anastopoulos I, Giannakoudakis DA, Lima EC (2021) Metal-organic and zeolitic imidazole frameworks as cationic dye adsorbents: physicochemical optimizations by parametric modeling and kinetic studies. J Mol Liq 332(June):115832. https://doi.org/10.1016/j.molliq.2021.115832

Chen G, Wang Y, Weng H, Wu Z, He K, Zhang P, Guo Z, Lin M (2019a) Selective separation of Pd(II) on pyridine-functionalized graphene oxide prepared by radiation-induced simultaneous grafting polymerization and reduction. ACS Appl Mater Interfaces 11(27):24560–24570. https://doi.org/10.1021/acsami.9b06162

Chen R, Tao CA, Zhang Z, Chen X, Liu Z, Wang J (2019b) Layer-by-layer fabrication of core-shell Fe3O4@UiO-66-NH2 with high catalytic reactivity toward the hydrolysis of chemical warfare agent simulants. ACS Appl Mater Interfaces 11(46):43156–43165. https://doi.org/10.1021/acsami.9b14099

Daliran S, Ghazagh-Miri M, Oveisi AR, Khajeh M, Navalón S, Âlvaro M, Ghaffari-Moghaddam M, Delarami HS, García H (2020) A pyridyltriazol functionalized zirconium metal-organic framework for selective and highly efficient adsorption of palladium. ACS Appl Mater Interfaces 12(22):25221–25232. https://doi.org/10.1021/acsami.0c06672

Donia AM, Atia AA, Elwakeel KZ (2007) Recovery of gold(III) and silver(I) on a chemically modified chitosan with magnetic properties. Hydrometallurgy 87(3–4):197–206. https://doi.org/10.1016/j.hydromet.2007.03.007

Dragan ES, Loghin DFA (2013) Enhanced sorption of methylene blue from aqueous solutions by semi-IPN composite cryogels with anionically modified potato starch entrapped in PAAm matrix. Chem Eng J 234:211–222. https://doi.org/10.1016/j.cej.2013.08.081

El Salam HMA, Zaki T (2018) Removal of hazardous cationic organic dyes from water using nickel-based metal-organic frameworks. Inorg Chim Acta 471:203–210. https://doi.org/10.1016/j.ica.2017.10.040

El-Shorbagy HG, El-Kousy SM, Elwakeel KZ, Abd El-Ghaffar MA (2021) Eco-friendly chitosan condensation adduct resins for removal of toxic silver ions from aqueous medium. Journal of Industrial and Engineering Chemistry, April 100:410–421. https://doi.org/10.1016/j.jiec.2021.04.029

Elwakeel KZ, El-Sayed GO, Darweesh RS (2013) Fast and selective removal of silver(I) from aqueous media by modified chitosan resins. Int J Miner Process 120:26–34. https://doi.org/10.1016/j.minpro.2013.02.007

Elwakeel KZ, Al-Bogami AS, Guibal E (2021) 2-Mercaptobenzimidazole derivative of chitosan for silver sorption – contribution of magnetite incorporation and sonication effects on enhanced metal recovery. Chem Eng J 403(May 2020):126265. https://doi.org/10.1016/j.cej.2020.126265

Embaby MS, Elwany SD, Setyaningsih W, Saber MR (2018) The adsorptive properties of UiO-66 towards organic dyes: a record adsorption capacity for the anionic dye alizarin red S. Chin J Chem Eng 26(4):731–739. https://doi.org/10.1016/j.cjche.2017.07.014

Far HS, Hasanzadeh M, Nashtaei MS, Rabbani M, Haji A, Moghadam BH (2020) PPI-dendrimer-functionalized magnetic metal-organic framework (Fe3O4@MOF@PPI) with high adsorption capacity for sustainable wastewater treatment. ACS Appl Mater Interfaces 12(22):25294–25303. https://doi.org/10.1021/acsami.0c04953

Guibal E, Von Offenberg Sweeney N, Vincent T, Tobin JM (2002) Sulfur derivatives of chitosan for palladium sorption. React Funct Polym 50(2):149–163. https://doi.org/10.1016/S1381-5148(01)00110-9

Hamedi A, Zarandi MB, Nateghi MR (2019) Highly efficient removal of dye pollutants by MIL-101(Fe) metal-organic framework loaded magnetic particles mediated by poly L-dopa. Journal of Environmental Chemical Engineering 7(1):102882. https://doi.org/10.1016/j.jece.2019.102882

Hasanzadeh M, Simchi A, Far HS (2019) Kinetics and adsorptive study of organic dye removal using water-stable nanoscale metal organic frameworks. Mater Chem Phys 233(May):267–275. https://doi.org/10.1016/j.matchemphys.2019.05.050

Hasanzadeh M, Simchi A, Far HS (2020) Nanoporous composites of activated carbon-metal organic frameworks for organic dye adsorption: synthesis, adsorption mechanism and kinetics studies. J Ind Eng Chem 81:405–414

Hayati B, Arami M, Maleki A, Pajootan E (2015) Thermodynamic properties of dye removal from colored textile wastewater by poly (propylene imine) dendrimer. Desalin Water Treat 56:97–106. https://doi.org/10.1080/19443994.2014.931529

Huang L, He M, Chen B, Bin H (2015) A designable magnetic MOF composite and facile coordination-based post-synthetic strategy for the enhanced removal of Hg2+ from water. J Mater Chem A 3(21):11587–11595. https://doi.org/10.1039/c5ta01484k

Huang L, He M, Chen B, Bin H (2016) A mercapto functionalized magnetic Zr-MOF by solvent-assisted ligand exchange for Hg2+ removal from water. J Mater Chem A 4(14):5159–5166. https://doi.org/10.1039/c6ta00343e

Huo J-B, Xu L, Chen X, Zhang Y, Yang J-CE, Yuan B, Ming-Lai F (2019) Direct epitaxial synthesis of magnetic Fe3O4@UiO-66 composite for efficient removal of arsenate from water. Microporous Mesoporous Mater 276(March):68–75. https://doi.org/10.1016/J.MICROMESO.2018.09.017

Iqbal M, Iqbal N, Bhatti IA, Ahmad N, Zahid M (2016) Response surface methodology application in optimization of cadmium adsorption by shoe waste: a good option of waste mitigation by waste. Ecol Eng 88(March):265–275. https://doi.org/10.1016/j.ecoleng.2015.12.041

Kanani-Jazi MH, Akbari S, Kish MH (2020) Efficient removal of Cr (VI) from aqueous solution by halloysite/poly(amidoamine) dendritic nano-hybrid materials: kinetic, isotherm and thermodynamic studies. Adv Powder Technol 31(9):4018–4030. https://doi.org/10.1016/j.apt.2020.08.004

Kayal S, Chakraborty A (2018) Activated carbon (type Maxsorb-III) and MIL-101(Cr) metal organic framework based composite adsorbent for higher CH4 storage and CO2 capture. Chem Eng J 334:780–788. https://doi.org/10.1016/j.cej.2017.10.080

Khan NA, Khan SU, Ahmed S, Farooqi IH, Dhingra A, Hussain A, Changani F (2019) Applications of nanotechnology in water and wastewater treatment: a review. Asian Journal of Water, Environment and Pollution 16(4):81–86. https://doi.org/10.3233/AJW190051

Khiarak BN, Hasanzadeh M, Mojaddami M, Far HS, Simchi A (2020) In situ synthesis of quasi-needle-like bimetallic organic frameworks on highly porous graphene scaffolds for efficient electrocatalytic water oxidation. Chem Commun 56(21):3135–3138. https://doi.org/10.1039/c9cc09908e

Kousha M, Daneshvar E, Esmaeli AR, Jokar M, Khataee AR (2012) Optimization of acid blue 25 removal from aqueous solutions by raw , esterified and protonated Jania adhaerens biomass. Int Biodeterior Biodegradation 69:97–105. https://doi.org/10.1016/j.ibiod.2012.01.007

Krawczyk M, Akbari S, Jeszka-Skowron M, Pajootan E, Fard FS (2016) Application of dendrimer modified halloysite nanotubes as a new sorbent for ultrasound-assisted dispersive micro-solid phase extraction and sequential determination of cadmium and lead in water Samples. J Anal At Spectrom 31(7):1505–1514. https://doi.org/10.1039/c6ja00096g

Li J, Wang S, Wang F, Xuran W (2019) Environmental separation and enrichment of gold and palladium ions by amino-modified three-dimensional graphene. RSC Adv 9(5):2816–2821. https://doi.org/10.1039/c8ra10506e

Li L, Xu Y, Zhong D, Zhong N (2020a) CTAB-surface-functionalized magnetic MOF@MOF composite adsorbent for Cr(VI) efficient removal from aqueous solution. Colloids Surf A Physicochem Eng

Asp 586(Vi):124255. https://doi.org/10.1016/j.colsurfa.2019.124255

Li Y, Wang Y, He L, Meng L, Lu H, Li X (2020b) Preparation of poly(4-vinylpyridine)-functionalized magnetic Al-MOF for the removal of naproxen from aqueous solution. J Hazard Mater 383(August 2019): 121144. https://doi.org/10.1016/j.jhazmat.2019.121144

Lim CR, Lin S, Yun YS (2020) Highly efficient and acid-resistant metal-organic frameworks of MIL-101(Cr)-NH2 for Pd(II) and Pt(IV) recovery from acidic solutions: adsorption experiments, spectroscopic analyses, and theoretical computations. J Hazard Mater 387(Ii): 121689. https://doi.org/10.1016/j.jhazmat.2019.121689

Lima EC, Hosseini-bandegharaei A, Moreno-piraján JC, Anastopoulos I (2019) A critical review of the estimation of the thermodynamic parameters on adsorption equilibria. Wrong use of equilibrium constant in the Van â€™ T Hoof equation for calculation of thermodynamic parameters of adsorption. J Mol Liq 273:425–434. https://doi.org/10.1016/j.molliq.2018.10.048

Lin S, Bediako JK, Cho CW, Song MH, Zhao Y, Kim JA, Choi JW, Yun YS (2018) Selective adsorption of Pd(II) over interfering metal ions (Co(II), Ni(II), Pt(IV)) from acidic aqueous phase by metal-organic frameworks. Chem Eng J 345(March):337–344. https://doi.org/10.1016/j.cej.2018.03.173

Lin S, Zhao Y, Bediako JK, Cho CW, Sarkar AK, Lim CR, Yun YS (2019) Structure-controlled recovery of palladium(II) from acidic aqueous solution using metal-organic frameworks of MOF-802, UiO-66 and MOF-808. Chem Eng J 362(October 2018):280–286. https://doi.org/10.1016/j.cej.2019.01.044

Liu Y, Liu YJ (2008) Biosorption isotherms, kinetics and thermodynamics. Sep Purif Technol 61(3):229–242. https://doi.org/10.1016/j.seppur.2007.10.002

Liu L, Li C, Bao C, Jia Q, Xiao P, Liu X, Zhang Q (2012) Preparation and characterization of chitosan/graphene oxide composites for the adsorption of Au(III) and Pd(II). Talanta 93:350–357. https://doi.org/10.1016/j.talanta.2012.02.051

Liu J, Zeng M, Ronghai Y (2016) Surfactant-free synthesis of octahedral ZnO / ZnFe 2 O 4 heterostructure with ultrahigh and selective adsorption capacity of malachite green. Nat Publ Group 2015:1–10. https://doi.org/10.1038/srep25074

Liu Q, Deng CH, Sun N (2018) Hydrophilic tripeptide-functionalized magnetic metal-organic frameworks for the highly efficient enrichment of N-linked glycopeptides. Nanoscale 10(25):12149–12155. https://doi.org/10.1039/c8nr03174f

Mergola L, Stomeo T, Del Sole R (2020) Synthesis of photoswitchable submicroparticles and their evaluation as ion-imprinted polymers for Pd(II) uptake. Polym J 52(7):743–754. https://doi.org/10.1038/s41428-020-0319-8

Mincke S, Asere TG, Verheye I, Folens K, Vanden Bussche F, Lapeire L, Verbeken K, Van Der Voort P (2019) Functionalized chitosan adsorbents allow recovery of palladium and platinum from acidic aqueous solutions. Green Chem 21(9):2295–2306. https://doi.org/10.1039/C9GC00166B

Moawed EA, El-Hagrasy MA, Kamal M, El-Shahat MF (2016) Recovery and determination of palladium from its alloys using iminodiacetic polyurethane/carbon nanofibers sorbent. J Liq Chromatogr Relat Technol 39(8):415–421. https://doi.org/10.1080/10826076.2016.1169428

Moghadam BH, Hasanzadeh M, Simchi A (2020) Self-powered wearable piezoelectric sensors based on polymer nanofiber-metal-organic framework nanoparticle composites for arterial pulse monitoring. ACS Applied Nano Materials 3(9):8742–8752. https://doi.org/10.1021/acsanm.0c01551

Moghaddam H, Masoumeh RN, Dehghani MH, Akbarpour B, Azari A, Yousefi M (2019) Performance investigation of zeolitic imidazolate framework – 8 (ZIF-8) in the removal of trichloroethylene from aqueous solutions. Microchem J 150(August):104185. https://doi.org/10.1016/j.microc.2019.104185

Mohammad N, Hayati B, Arami M, Lan C (2011) Adsorption of textile dyes on pine cone from colored wastewater : kinetic , equilibrium and thermodynamic studies. Desalination 268(1–3):117–125. https://doi.org/10.1016/j.desal.2010.10.007

Molavi H, Shojaei A, Pourghaderi A (2018) Rapid and Tunable Selective adsorption of dyes using thermally oxidized nanodiamond. J Colloid Interface Sci 524:52–64. https://doi.org/10.1016/j.jcis.2018.03.088

Myers RH, Montgomery DC, Anderson-cook CM (2009) *Response surface methodology: process and product optimization using designed experiments*. John Wiley and Sons, USA

Nagarjuna R, Shivani S, Rajesh N, Ganesan R (2017) Effective adsorption of precious metal palladium over polyethyleneimine-functionalized alumina nanopowder and its reusability as a catalyst for energy and environmental applications. ACS Omega 2(8):4494–4504. https://doi.org/10.1021/acsomega.7b00431

Natale F, Di M, Orefice FLM, Erto A, Lancia A (2017) Unveiling the potentialities of activated carbon in recovering palladium from model leaching solutions. Sep Purif Technol 174:183–193. https://doi.org/10.1016/j.seppur.2016.10.022

Oladipo AA, Gazi M, Saber-samandari S (2014) Adsorption of anthraquinone dye onto eco-friendly semi-IPN biocomposite hydrogel : equilibrium isotherms, kinetic studies and optimization. J Taiwan Inst Chem Eng 45(2):653–664. https://doi.org/10.1016/j.jtice.2013.07.013

Parajuli D, Kawakita H, Inoue K, Funaoka M (2006) Recovery of gold(III), palladium(II), and platinum(IV) by aminated lignin derivatives. Ind Eng Chem Res 45(19):6405–6412. https://doi.org/10.1021/ie0603518

Qiu J, Feng Y, Zhang X, Jia M, Yao J (2017) Acid-promoted synthesis of UiO-66 for highly selective adsorption of anionic dyes: adsorption performance and mechanisms. J Colloid Interface Sci 499(March): 151–158. https://doi.org/10.1016/j.jcis.2017.03.101

Ramesh A, Hasegawa H, Sugimoto W, Maki T, Ueda K (2008) Adsorption of gold(III), platinum(IV) and palladium(II) onto glycine modified crosslinked chitosan resin. Bioresour Technol 99(9): 3801–3809. https://doi.org/10.1016/j.biortech.2007.07.008

Senosy IA, Lu ZH, Abdelrahman TM, Yang MNO, Guo HM, Yang ZH, Li JH (2020) The post-modification of magnetic metal-organic frameworks with β-cyclodextrin for the efficient removal of fungicides from environmental water. Environmental Science: Nano 7(7): 2087–2101. https://doi.org/10.1039/c9en01372e

Sharifi S, Nabizadeh R, Akbarpour B, Azari A, Ghaffari HR, Nazmara S, Mahmoudi B, Shiri L, Yousefi M (2019) Modeling and optimizing parameters affecting hexavalent chromium adsorption from aqueous solutions using Ti-XAD7 nanocomposite: RSM-CCD approach, kinetic, and isotherm studies. J Environ Health Sci Eng 17(2):873–888. https://doi.org/10.1007/s40201-019-00405-7

Sharma S, Wu CM, Koodali RT, Rajesh N (2016) An ionic liquid-mesoporous silica blend as a novel adsorbent for the adsorption and recovery of palladium ions, and its applications in continuous flow study and as an industrial catalyst. RSC Adv 6(32):26668–26678. https://doi.org/10.1039/c5ra26673d

Wu MX, Gao J, Wang F, Yang J, Song N, Jin X, Mi P, Tian J, Luo J, Liang F, Yang Y-W (2018) Multistimuli responsive core–shell nanoplatform constructed from Fe3O4@MOF equipped with Pillar[6]arene nanovalves. Small 14(17):1–6. https://doi.org/10.1002/smll.201704440

Yang J, Zhang Z, Pang W, Chen H, Yan G (2019) Polyamidoamine dendrimers functionalized magnetic carbon nanotubes as an efficient adsorbent for the separation of flavonoids from plant extraction. Sep Purif Technol 227(March):115710. https://doi.org/10.1016/j.seppur.2019.115710

Yen CH, Lien HL, Chung JS, Der Yeh H (2017) Adsorption of precious metals in water by dendrimer modified magnetic nanoparticles. J Hazard Mater 322(February):215–222. https://doi.org/10.1016/j.jhazmat.2016.02.029

Yi Q, Fan R, Xie F, Zhang Q, Luo Z (2016) Recovery of palladium(II) from nitric acid medium using a natural resin prepared from persimmon dropped fruits residues. J Taiwan Inst Chem Eng 61:299–305. https://doi.org/10.1016/j.jtice.2016.01.009

Zhang B, Likang F, Wang S, Zhang L (2018) Adsorption of palladium(II) from aqueous solution using nanosilica modified with imidazoline groups. Mater Chem Phys 214(Ii):533–539. https://doi.org/10.1016/j.matchemphys.2018.04.120

Zhang W, Hu L, Hu S, Yang L (2019) Optimized synthesis of novel hydrogel for the adsorption of copper and cobalt ions in wastewater. RSC Adv 9(28):16058–16068. https://doi.org/10.1039/c9ra00227h

Zhang X, Wang J, Dong XX, Lv YK (2020) Functionalized metal-organic frameworks for photocatalytic degradation of organic pollutants in environment. Chemosphere 242. https://doi.org/10.1016/j.chemosphere.2019.125144

Zhao X, Liu S, Tang Z, Niu H, Cai Y, Meng W, Wu F, Giesy JP (2015) Synthesis of magnetic metal-organic framework (MOF) for efficient removal of organic dyes from water. Sci Rep 5(July):1–10. https://doi.org/10.1038/srep11849

Zhou L, Liu J, Liu Z (2009) Adsorption of platinum(IV) and palladium(II) from aqueous solution by thiourea-modified chitosan microspheres. J Hazard Mater 172(1):439–446. https://doi.org/10.1016/j.jhazmat.2009.07.030

Zhou L, Xu J, Liang X, Liu Z (2010) Adsorption of platinum(IV) and palladium(II) from aqueous solution by magnetic cross-linking chitosan nanoparticles modified with ethylenediamine. J Hazard Mater 182(1–3):518–524. https://doi.org/10.1016/j.jhazmat.2010.06.062